CrystEngComm

A New Alkaline Beryllium Borate KBe4B3O9 with ribbon alveolate [Be2BO5]∞ layers and the structural evolution of ABe4B3O9 (A = K, Rb and Cs)

Journal:	*CrystEngComm*
Manuscript ID:	CE-ART-01-2014-000085.R1
Article Type:	Paper
Date Submitted by the Author:	14-Feb-2014
Complete List of Authors:	Ye, Ning; Fujian Institute of Research on the Structure of Matter, Wang, Shichao; Northwestern University, Chemistry zou, guohong; Fujian Institute of Research on the Structure of MatterChinese Academy of Sciences,

A New Alkaline Beryllium Borate $KBe_4B_3O_9$ with ribbon alveolate $[Be_2BO_5]_\infty$ layers and the structural evolution of $ABe_4B_3O_9$ (A = K, Rb and Cs)

Shichao Wang, Ning Ye* and Guohong Zou
Key Laboratory of Optoelectronic Materials Chemistry and Physics,
Fujian Institute of Research on the Structure of Matter,
Chinese Academy of Sciences, Fuzhou, Fujian, 350002, P. R. China
Email: nye@fjirsm.ac.cn

Abstract

The new alkaline beryllium borate $KBe_4B_3O_9$ was synthesized by spontaneous crystallization with molten fluxes based on K_2O–B_2O_3 solvent for the first time. From single crystal X-ray diffraction measurement $KBe_4B_3O_9$ has been found to crystallize in the monoclinic space group *P2/c*. $KBe_4B_3O_9$ consist of 2D ribbon alveolate beryllium borate $[Be_2BO_5]_\infty$ layers which are connected directly by strong covalent bonds. The structural evolution of $ABe_4B_3O_9$ (A = K, Rb and Cs) was discussed. The UV–Vis diffuse reflectance spectroscopy on powder samples indicated that the short-wavelength absorption edges of aforementioned materials are all below 200 nm. A new method is reported for the synthesis of $RbBe_4B_3O_9$ and $CsBe_4B_3O_9$. Thermal behavior of $KBe_4B_3O_9$ and $RbBe_4B_3O_9$ demonstrates that they are all incongruently melting compounds.

Introduction

Borates have been attracted more attention over the past decades because of their rich structural chemistry and increasing demand in many applications, such as nonlinear optical (NLO), birefringent optics, electrode materials, and other useful properties.[1, 2] The most important application of borate crystals is their use as ultraviolet (UV) nonlinear optical crystals for laser frequency conversion by the second harmonic genetation (SHG) due to their unique UV transparency and high damage threshold.[3-5] Over the years, several important UV NLO crystals have been discovered, including β-BaB_2O_4 (BBO)[6], LiB_3O_5 (LBO)[7], CsB_3O_5 (CBO)[8] and $CsLiB_6O_{10}$ (CLBO)[9, 10]. In particular, beryllium borates have played an important role in deep ultraviolet (deep UV) optical crystals, because they possess a very large energy gap as long as the A-site cations are alkaline or alkaline earth metals.[11] Typical examples of beryllium borate frameworks are the two-dimensional (2D) $[Be_2BO_3F_2]_\infty$ layers that can be found in $ABe_2BO_3F_2$ (A = Na, K, Rb, Cs and Tl)[12-17] and 2D $[Be_3B_3O_6]_\infty$ layers that can be found in $M_2Be_2B_2O_7$ (M = Sr and Ba)[18, 19]; among which, KBBF ($KBe_2BO_3F_2$)[15] has been shown to be the best material for deep UV applications and is the only material that can generate coherent light at 170 nm by direct SHG. However, this crystal has a very strong layer habit with respect to crystal growth due to the relatively weak F^-–K^+ ionic interactions between the adjacent $[Be_2BO_3F_2]_\infty$ layers along the *c*-axis.[20, 21]

In our previous study, we reported the discovery of four deep UV NLO crystals that include β-$KBe_2B_3O_7$, γ-$KBe_2B_3O_7$, $RbBe_2B_3O_7$[22] and $Na_2CsBe_6B_5O_{15}$[23] which

consist of 2D $[Be_2BO_5]_\infty$ layers connected by strong covalent bonds. This approach to beryllium borate construction and various types of framework connection was successful and will allow further advances in UV optical materials development.

In this study, we have carried out a systematic synthesis based on the $A_2O–BeO–B_2O_3$ (A = K, Rb, Cs) quaternary system to obtain UV optical crystals containing $[Be_2BO_5]_\infty$ layers. This has resulted in a series of alkaline beryllium borates with the general formula $ABe_4B_3O_9$. The synthesis, crystal structure and properties of $KBe_4B_3O_9$ are reported here for the first time. The Rb^+ and Cs^+ analogues, $RbBe_4B_3O_9$[24] and $CsBe_4B_3O_9$[25], which have been reported previously are also discussed in this work in terms of an improved synthetic methodology and property characterization. The thermal behavior and optical properties of $RbBe_4B_3O_9$ have been analyzed for the first time.

Experimental Section

Reagents

K_2CO_3 (99.8%), Rb_2CO_3 (99.5%), Cs_2CO_3 (99.9%), BeO (99.5%), and B_2O_3 (99.5%) were purchased from Sinopharm and used as received. Due to the toxicity of BeO, all of the experiments were performed in a ventilated system.

Crystal Growth

$KBe_4B_3O_9$: Single crystals of $KBe_4B_3O_9$ were grown from a high temperature solution by using $K_2O–3B_2O_3$ as a flux. This solution was prepared in a platinum crucible by melting a mixture of K_2CO_3, BeO and B_2O_3 at molar ratio of K_2O : BeO : B_2O_3 = 1 : 1 : 3. The mixture (10 g) was heated in a programmable temperature

electric furnace with a thermal field of high symmetry and stability at 900 °C until the melt became transparent and clear. The homogenized melt solution was then cooled rapidly (50 °C/h) to the initial crystallization temperature (850 °C). It was further cooled slowly (3 °C/h) to the final crystallization temperature (750 °C), then allowed to cool to room temperature by powering off the furnace.

$RbBe_4B_3O_9$: Single crystals of $RbBe_4B_3O_9$ were grown from a high temperature solution by using $Rb_2O–2B_2O_3$ as a flux. This solution was prepared in a platinum crucible by melting a mixture of Rb_2CO_3, BeO and B_2O_3 at molar ratio of Rb_2O : BeO : B_2O_3 = 1 : 1 : 2. The mixture (10 g) was heated in a programmable temperature electric furnace with a thermal field of high symmetry and stability at 900 °C until the melt became transparent and clear. The homogenized melt solution was then cooled rapidly (50 °C/h) to the initial crystallization temperature (750 °C). It was further cooled slowly (3 °C/h) to the final crystallization temperature (650 °C), then allowed to cool to room temperature by powering off the furnace.

$CsBe_4B_3O_9$: Single crystals of $CsBe_4B_3O_9$ were grown from a high temperature solution by using $Cs_2O–2B_2O_3$ as a flux. This solution was prepared in a platinum crucible by melting a mixture of Cs_2CO_3, BeO and B_2O_3 at molar ratio of Cs_2O : BeO : B_2O_3 = 1 : 1 : 2. The mixture (10 g) was heated in a programmable temperature electric furnace with a thermal field of high symmetry and stability at 800 °C until the melt became transparent and clear. The homogenized melt solution was then cooled rapidly (50 °C/h) to the initial crystallization temperature (750 °C). It was further cooled slowly (3 °C/h) to the final crystallization temperature (650 °C), then allowed

to cool to room temperature by powering off the furnace. The flux attached to the crystal was readily dissolved in water.

Single Crystal X-ray Diffraction

Single crystal X-ray diffraction data were collected at room temperature on a Rigaku Mercury CCD diffractometer with graphite-monochromatic Mo Kα radiation (λ = 0.71073 Å). A transparent block of crystal was mounted on a glass fiber with epoxy for structure determination. A hemisphere of data was collected using a narrow-frame method with the ω-scan mode. The data were integrated using the CrystalClear program, and the intensities were corrected for Lorentz polarization, air absorption, and absorption attributable to the variation in the path length through the detector faceplate. Absorption corrections based on the Multiscan technique were also applied. The structure was solved by direct methods using SHELXS-97 and then refined by full-matrix least-squares refinement on F^2 with SHELXL-97[26] found in the software suite WinGX[27] v1.80.05. All of the structures were verified using ADDSYM algorithm from the program PLATON[28], and no higher symmetries were found. Relevant crystallographic data and details of the experimental conditions for $KBe_4B_3O_9$, $RbBe_4B_3O_9$ and $CsBe_4B_3O_9$ are summarized in Table 1 and Table S1. Atomic coordinates and isotropic displacement coefficients are listed in Table 2 and S2−S3.

Powder X-ray Diffraction

X-ray diffraction patterns of polycrystalline materials were obtained on a Rigaku Dmax2500 powder X-ray diffractometer by using Cu Kα radiation (λ = 1.540598 Å)

at room temperature in the angular range of 2θ = 0–60° with a scan step width of 0.05° and a fixed time of 0.2 s. The powder XRD patterns for $KBe_4B_3O_9$, $RbBe_4B_3O_9$ and $CsBe_4B_3O_9$, showed good agreement with the calculated XRD patterns from the single crystal models.

Elemental Analysis

Elemental analysis of the crystals was performed by using a Jobin Yvon Ultima2 inductively coupled plasma optical emission spectrometer (ICP–OES) with Sepex Certiprep standards. The crystal samples were dissolved in a mixture of nitric acid (3 mL) and hydrochloric acid (3 mL).

Differential Thermal Analysis

Differential thermal analysis (DTA) scans were measured on a NETZSCH STA 449C simultaneous analyzer. Reference (Al_2O_3) and crystal samples (5–15 mg) were enclosed in Al_2O_3 crucibles and heated from room temperature to 1100 °C at a rate of 15 °C/min under a constant flow of nitrogen gas. The DTA residues were visually inspected and then analyzed by X-ray powder diffraction after the experiments.

UV–Vis Diffuse Reflectance Spectroscopy

The UV–Vis diffuse reflection spectra were recorded at room temperature using a powder sample with $BaSO_4$ as a standard (100% reflectance) on a PerkinElmer Lamda-900 UV/Vis/NIR Spectrophotometer over the spectra range 200–800 nm. Reflectance spectra were converted to absorbance using the Kubelka–Munk function.[29, 30]

Results and discussion

Thermal Behavior and Crystal Growth

We have successfully synthesized a new series of alkaline beryllium borate crystals of $ABe_4B_3O_9$ (A = K, Rb and Cs) based on the A_2O–BeO–B_2O_3 (A = K, Rb and Cs) system. As shown in Fig 1, the DTA curves for $KBe_4B_3O_9$ exhibit only one endothermic peak beginning at 1014 °C upon heating to 1100 °C. Analysis of the powder XRD pattern of the DTA residues revealed that $KBe_4B_3O_9$ was decomposed into $Be_3B_2O_6$[31] and BeO, demonstrating that $KBe_4B_3O_9$ is an incongruently melting compound. Therefore, large crystals of $KBe_4B_3O_9$ must be grown with flux and below the decomposition temperature.

Although the compound of $RbBe_4B_3O_9$ has been studied previously, no thermal property was reported. As shown in Fig 2, the DTA curves for $RbBe_4B_3O_9$ exhibit only one endothermic peak beginning at 1003 °C upon heating to 1100 °C. Analysis of the powder XRD pattern of the DTA residues revealed that $RbBe_4B_3O_9$ was decomposed into $Be_3B_2O_6$[31] and BeO, demonstrating that $RbBe_4B_3O_9$ is an incongruently melting compound. Therefore, large crystals of $RbBe_4B_3O_9$ must be grown with flux and below the decomposition temperature. The DTA curves for $CsBe_4B_3O_9$ measured here (Fig S1) is the same with the previous reported, which exhibit only one endothermic peak beginning at 921 °C upon heating. Above this temperature, $CsBe_4B_3O_9$ was decomposed into $Be_3B_2O_6$[31] and BeO, demonstrating that $CsBe_4B_3O_9$ is an incongruently melting compound.

The previously described method for the synthesis of $RbBe_4B_3O_9$ and $CsBe_4B_3O_9$ tends to introduce many complex starting materials. For example,

$RbBe_4B_3O_9$ was grown by BeF_2, BeO, Rb_2CO_3, NaF and B_2O_3; $CsBe_4B_3O_9$ was grown by Cs_2CO_3, Li_2CO_3, BeO and B_2O_3. The new method we reported here is an easy way to simplify the reaction system and improve the quality of the isolated crystals. Hence, as shown in Fig 3, transparent and colorless $KBe_4B_3O_9$, $RbBe_4B_3O_9$ and $CsBe_4B_3O_9$ crystals have been grown by spontaneous crystallization in a molten flux based on the self-fluxed system $A_2O–B_2O_3$, which has low melting temperature and good solubility for beryllium borate compounds. They are all chemically stable with respect to water and air.

Crystal Structure

$KBe_4B_3O_9$ crystallizes in monoclinic crystal system with a centrosymmetric space group of *P2/c*. The structure is illustrated along the *b*-axis in Fig 4. The B atoms are coordinated to three O atoms to form planar [BO_3] triangles with B–O bond lengths ranging from 1.3380(16) to 1.4124(17) Å and O–B–O bond angles ranging from 115.30(11) to 123.04(12)°. The Be atoms are bound to four O atoms to form distorted [BeO_4] tetrahedra with Be–O bond lengths ranging from 1.6017(19) to 1.6767(18) Å and O–Be–O bond angles from 104.45(10) to 115.78(11)°. All O atoms are three coordinated except O5 atom, which is two coordinated. The 2D alveolate beryllium borate $[Be_2BO_5]_\infty$ layers in this structure are similar to those in β-$KBe_2B_3O_7$, $RbBe_2B_3O_7$, γ-$KBe_2B_3O_7$ and $Na_2CsBe_6B_5O_{15}$, except that the adjacent $[Be_2BO_5]_\infty$ layers are connected directly by Be1–O4 and Be2–O5 bond in the layers. As a result, the ribbon $[Be_2BO_5]_\infty$ layers extend infinitely along the *b*-axis, but they are cut off along the other direction on edge. The adjacent $[Be_2BO_5]_\infty$ layers align parallel to

each other from opposite direction. One type of tunnel exists in the 3D framework running along the *b*-axis. The K^+ cations reside in these tunnels, where K^+ cations are located in a ten-coordinate environment with K–O bond lengths ranging from 2.7927(13) to 3.0732(15) Å. Although $KBe_4B_3O_9$ contains NLO–active $[Be_2BO_5]_\infty$ layers, their centrosymmetric alignment results in the cancellation of NLO susceptibilities.

$RbBe_4B_3O_9$ and **$CsBe_4B_3O_9$** are isostructural and crystallize in orthorhombic crystal system with a centrosymmetric space group of *Pnma*. It is worthwhile to note that our structure refinements agree well with those found in the study by Wen and Huang.

Fig S2–S4 show the X-ray powder diffraction patterns of $KBe_4B_3O_9$, $RbBe_4B_3O_9$ and $CsBe_4B_3O_9$. The peak positions match the theoretical patterns simulated from single crystal refinements.

The results of ICP elemental analysis of $KBe_4B_3O_9$ (Table S4) were consistent with the compositions determined from single crystal X-ray analysis.

The effect of cation on assembly of the beryllium borate units

It is worth comparing the structure of $KBe_4B_3O_9$, $RbBe_4B_3O_9$ and $CsBe_4B_3O_9$ because of the formula and structural similarity. $RbBe_4B_3O_9$ and $CsBe_4B_3O_9$ are isostructural. Although $KBe_4B_3O_9$ adopts the different structure from $ABe_4B_3O_9$ (A = Rb and Cs), they all have the common $[Be_2BO_5]_\infty$ layers. Because there is only one unique orientation of $[BO_3]^{3-}$ groups in the $[Be_2BO_5]_\infty$ layers of $KBe_4B_3O_9$ and $ABe_4B_3O_9$ (A = Rb and Cs), the evolution of structure between them can be clearly

explained by showing the structures with $[BO_3]^{3-}$ groups oriented to the same direction. In the symmetric unit of $ABe_4B_3O_9$ (A = K, Rb and Cs), A, Be, B, and O occupy one, two, two, and five crystallographically unique positions, respectively. For the sake of discussion, atoms were uniformly labeled in Fig 5. The $ABe_4B_3O_9$ (A = K, Rb and Cs) all consist of 2D ribbon $[Be_2BO_5]_\infty$ layers which are connected with each other directly by strong covalent bonds. The orientations of the $[BeO_4]$ tetrahedra in the ribbon $[Be_2BO_5]_\infty$ layers result in the different connection between the adjacent $[Be_2BO_5]_\infty$ layers from $KBe_4B_3O_9$ to $ABe_4B_3O_9$ (A = Rb and Cs). The layers are bridged by Be1−O4 and Be2−O5 bond in $KBe_4B_3O_9$, while the connections are Be1−O5 and Be2−O4 bond in $ABe_4B_3O_9$ (A = Rb and Cs).

The effect of cation size on the overall structure has been observed in $ABe_4B_3O_9$ (A = K, Rb and Cs). Compared with larger Rb^+ and Cs^+, K^+ takes smaller cation size. The requirement of K^+ for ten-fold coordination environment with K−O bond lengths ranging from 2.7927(13) to 3.0732(15) Å leads to the relatively compact connection of flat $[Be_2BO_5]_\infty$ layers in $KBe_4B_3O_9$. The distances between adjacent layers in $KBe_4B_3O_9$ are 5.25 Å, so that small K^+ cation can be accommodated in these tunnels. In $RbBe_4B_3O_9$, the ten-fold coordination environment of Rb^+ with Rb−O bond lengths ranging from 2.9912(16) to 3.443(2) Å results in the formation of a distortion of $[Be_2BO_5]_\infty$ layers along *a*-*b* plane to accommodate a large Rb^+ cation. Meanwhile, more appropriate orientations of the $[BeO_4]$ tetrahedra are adjusted in the ribbon $[Be_2BO_5]_\infty$ layers. In $CsBe_4B_3O_9$, the eleven-fold coordination environment of Cs^+ with Cs−O bond lengths ranging from 3.091(2) to 3.565(2) Å results in a more

distorted of $[Be_2BO_5]_\infty$ layers to generate bigger cages 6.45 Å in diameter, which is 6.28 Å in $RbBe_4B_3O_9$. It is readily seen that the $[Be_2BO_5]_\infty$ layer is flexible enough to accommodate the aforementioned alkaline cation. The structural evolution of these alkaline beryllium borates is determined by the interactions between the $[Be_2BO_5]_\infty$ layer and the alkali metal with different cation size.

Optical Properties

UV−Vis diffuse reflectance spectra were collected for $ABe_4B_3O_9$ (A = K, Rb and Cs) shown in Fig S5−S7. Absorption (K/S) data were calculated from the following Kubelka−Munk function:[29, 30] $F(R) = (1-R)^2/2R = K/S$, where R is the reflectance, K is the absorption, and S is the scattering. In the (K/S) versus E plots, extrapolating the linear part of the rising curve to zero provided the onset of absorption. No obvious absorption peak in the range of 6.22−1.55eV (corresponding to 200−800 nm) was observed for $KBe_4B_3O_9$, $RbBe_4B_3O_9$ and $CsBe_4B_3O_9$.

Conclusions

A series of alkaline beryllium borates $ABe_4B_3O_9$ (A = K, Rb and Cs) has been grown by spontaneous crystallization with molten flux based on $A_2O-B_2O_3$ (A = K, Rb and Cs) solvent. New compound $KBe_4B_3O_9$ crystallizes in the monoclinic space group *P2/c*. $KBe_4B_3O_9$ consist of 2D alveolate beryllium borate $[Be_2BO_5]_\infty$ layers which are connected directly by strong covalent bonds. The effect of cation size results in the structural evolution of $ABe_4B_3O_9$. The DTA curves suggest that $KBe_4B_3O_9$ and $RbBe_4B_3O_9$ are all incongruently melting compounds. The UV−Vis diffuse reflectance spectroscopy on powder samples indicated that the

short-wavelength absorption edges of these centrosymmetric compounds are all below 200 nm. Our further research efforts will be devoted to the explorations of other new UV crystals.

Acknowledgements

This research was supported by the National Natural Science Foundation of China (Nos. 91222204 and 90922035), Main Direction Program of Knowledge Innovation of Chinese Academy of Sciences (Grant No. KJCX2-EW-H03-03) and Special Project of National Major Scientific Equipment Development of China (No. 2012YQ120060).

Electronic supplementary information (ESI) available: X-ray crystallographic files in CIF format, DTA curves, simulated and measured powder XRD patterns, diffuse reflectance absorption curves.

References

1. P. Becker, *Adv. Mater.*, 1998, **10**, 979.
2. P. S. Halasyamani and K. R. Poeppelmeier, *Chem. Mater.*, 1998, **10**, 2753.
3. H. W. Yu, H. P. Wu, S. L. Pan, Z. H. Yang, X. Su and F. F. Zhang, *J. Mater. Chem.*, 2012, **22**, 9665.
4. H. P. Wu, H. W. Yu, S. L. Pan, Z. J. Huang, Z. H. Yang, X. Su and K. R. Poeppelmeier, *Angew. Chem.-Int. Edit.*, 2013, **52**, 3406.
5. H. P. Wu, H. W. Yu, Z. H. Yang, X. L. Hou, X. Su, S. L. Pan, K. R. Poeppelmeier and J. M. Rondinelli, *J. Am. Chem. Soc.*, 2013, **135**, 4215.
6. C. T. Chen, B. C. Wu, A. D. Jiang and G. M. You, *Sci. Sin. Ser. B*, 1985, **28**, 235.
7. C. T. Chen, Y. C. Wu, A. D. Jiang, B. C. Wu, G. M. You, R. K. Li and S. J. Lin, *J. Opt. Soc. Am. B*, 1989, **6**, 616.
8. Y. C. Wu, T. Sasaki, S. Nakai, A. Yokotani, H. G. Tang and C. T. Chen, *Appl. Phys. Lett.*, 1993, **62**, 2614.
9. Y. Mori, I. Kuroda, S. Nakajima, T. Sasaki and S. Nakai, *Appl. Phys. Lett.*, 1995, **67**, 1818.
10. J. M. Tu and D. A. Keszler, *Mater. Res. Bull.*, 1995, **30**, 209.
11. R. K. Li, *J. Non-Cryst. Solids*, 1989, **111**, 199.
12. L. F. Mei, Y. B. Wang and C. T. Chen, *Mater. Res. Bull.*, 1994, **29**, 81.
13. L. Mei, X. Huang, Y. Wang, Q. Wu, B. Wu and C. Chen, *Z. Kristall.*, 1995, **210**, 93.
14. C. T. Chen, S. Y. Luo, X. Y. Wang, G. L. Wang, X. H. Wen, H. X. Wu, X. Zhang and Z. Y. Xu, *J. Opt. Soc. Am. B*, 2009, **26**, 1519.

15. C. T. Chen, G. L. Wang, X. Y. Wang and Z. Y. Xu, *Appl. Phys. B: Lasers Opt.*, 2009, **97**, 9.
16. C. D. McMillen, J. Hu, D. VanDerveer and J. W. Kolis, *Acta Crystallogr. Sect. B: Struct. Sci.*, 2009, **65**, 445.
17. H. W. Huang, C. T. Chen, X. Y. Wang, Y. Zhu, G. L. Wang, X. Zhang, L. R. Wang and J. Y. Yao, *J. Opt. Soc. Am. B*, 2011, **28**, 2186.
18. C. T. Chen, Y. B. Wang, B. C. Wu, K. C. Wu, W. L. Zeng and L. H. Yu, *Nature*, 1995, **373**, 322.
19. H. Qi and C. T. Chen, *Chem. Lett.*, 2001, 352.
20. C. T. Chen, L. Bai, Z. Z. Wang and R. K. Li, *J. Cryst. Growth*, 2006, **292**, 169.
21. J. Q. Yu, L. J. Liu, S. F. Jin, H. T. Zhou, X. L. He, C. L. Zhang, W. N. Zhou, X. Y. Wang, X. L. Chen and C. T. Chen, *J. Solid State Chem.*, 2011, **184**, 2790.
22. S. C. Wang, N. Ye, W. Li and D. Zhao, *J. Am. Chem. Soc.*, 2010, **132**, 8779.
23. S. C. Wang and N. Ye, *J. Am. Chem. Soc.*, 2011, **133**, 11458.
24. X. H. Wen, R. K. Li and C. T. Chen, *Acta Crystallogr. Sect. C: Cryst. Struct. Commun.*, 2006, **62**, I21.
25. H. W. Huang, W. J. Yao, R. He, C. T. Chen, X. Y. Wang and Y. H. Zhang, *Solid State Sci.*, 2013, **18**, 105.
26. G. M. Sheldrick, *Acta Crystallographica Section A*, 2008, **64**, 112.
27. L. J. Farrugia, *J. Appl. Crystallogr.*, 1999, **32**, 827.
28. A. L. Spek, *J. Appl. Crystallogr.*, 2003, **36**, 7.
29. P. Kubelka and F. Munk, *Z. Tech. Phys*, 1931, **12**, 593.
30. J. Tauc, *Mater. Res. Bull.*, 1970, **5**, 721.
31. Blackbur.Pe and A. Buchler, *J. Phys. Chem.*, 1965, **69**, 4250.

Table 1. Crystal Data and Structure Refinement for $KBe_4B_3O_9$, $RbBe_4B_3O_9$ and $CsBe_4B_3O_9$

Formula	$KBe_4B_3O_9$
Formula Mass(amu)	251.57
Crystal System	Monoclinic
Space Group	*P2/c*
a (Å)	6.065(3)
b (Å)	4.463(2)
c (Å)	11.550(6)
β(°)	90.081(6)
V(Å^3)	312.6(3)
Z	2
Crystal Size (mm)	0.4×0.2×0.05
ρ(calcd)(g/cm^3)	2.673
Temperature(K)	293(2)
λ(Å)	0.71073
F(000)	244
μ(mm^{-1})	0.881
θ (deg)	3.36-27.35
Index Range	-7≤h≤7
	-5≤k≤5
	-14≤l≤14
R_{int}	0.0115
Reflections Collected	2108
Reflections(I>2σ(I))/ Independent Reflections	678/705
Data/Restraints/Parameters	705/0/81
R/wR (I>2σ (I))	0.0194/0.0544
R/wR (all data)	0.02/0.0548
GOF on F^2	1.131
Largest Diff. Peak and Hole (e/Å^{-3})	0.274 and -0.212

$R(F) = \Sigma||F_o| - |F_c||/\Sigma|F_o|$. $wR(F_o^2) = [\Sigma w(F_o^2 - F_c^2)^2/\Sigma w(F_o^2)^2]^{1/2}$.

Table 2. Atomic Positions and Isotropic Displacement Factors for $KBe_4B_3O_9$

atom	x	y	z	Wyckoff	$U_{eq}(Å^2)$	occupancy
K	0	0.25958(9)	1/4	2e	0.01177(16)	1
Be(1)	0.5199(3)	0.3393(4)	0.37289(13)	4g	0.0061(3)	1
Be(2)	-0.2304(3)	0.8250(4)	0.43886(13)	4g	0.0062(3)	1
B(1)	-1/2	-0.1622(5)	1/4	2f	0.0055(4)	1
B(2)	0.1923(2)	0.6542(3)	0.46090(11)	4g	0.0056(3)	1
O(1)	-1/2	0.1478(3)	1/4	2f	0.0063(3)	1
O(2)	-0.40084(14)	0.6834(2)	0.33840(7)	4g	0.0064(2)	1
O(3)	-0.28881(14)	0.1784(2)	0.45065(7)	4g	0.0061(2)	1
O(4)	0.28679(13)	0.3693(2)	0.44171(7)	4g	0.0058(2)	1
O(5)	0.01706(14)	0.7487(2)	0.40059(8)	4g	0.0073(2)	1

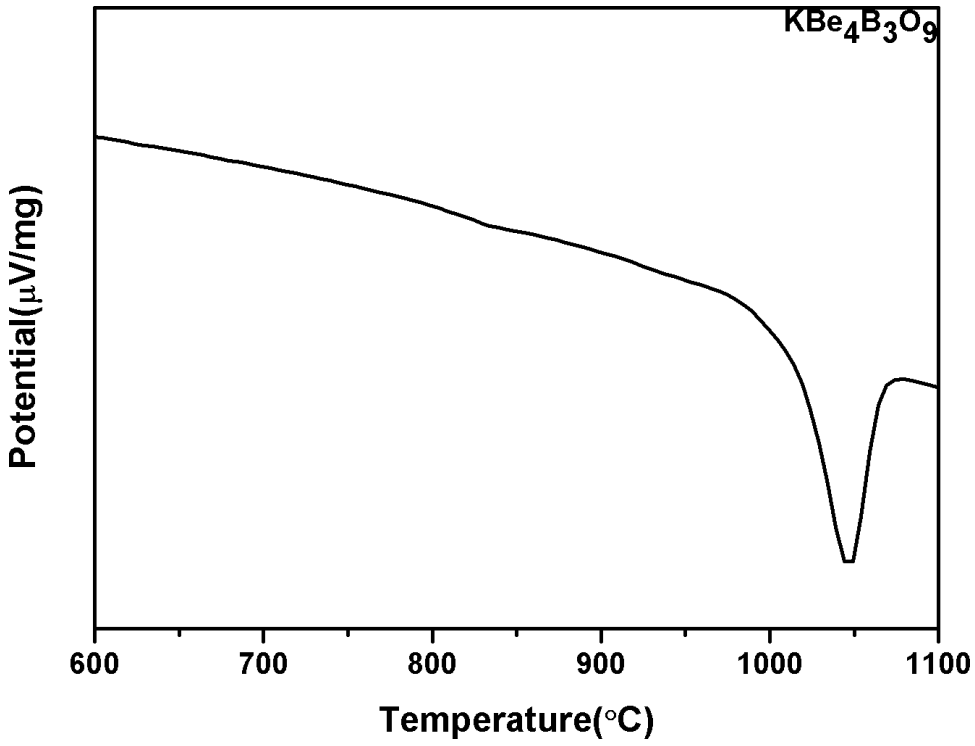

Fig 1. DTA trace for the compositions of $KBe_4B_3O_9$

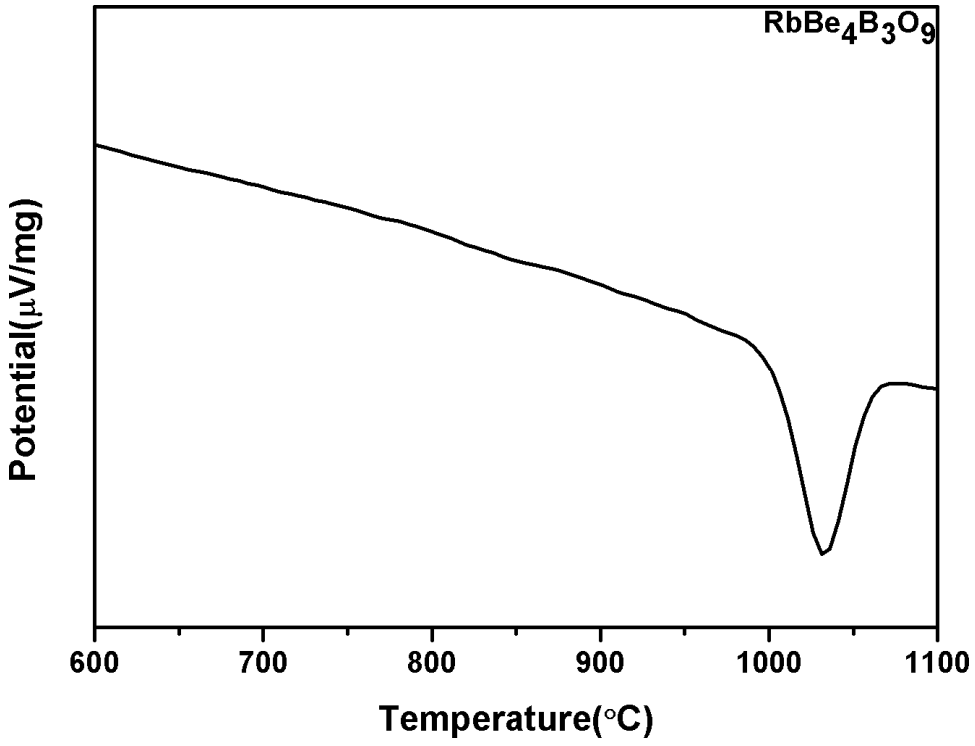

Fig 2. DTA trace for the compositions of $RbBe_4B_3O_9$

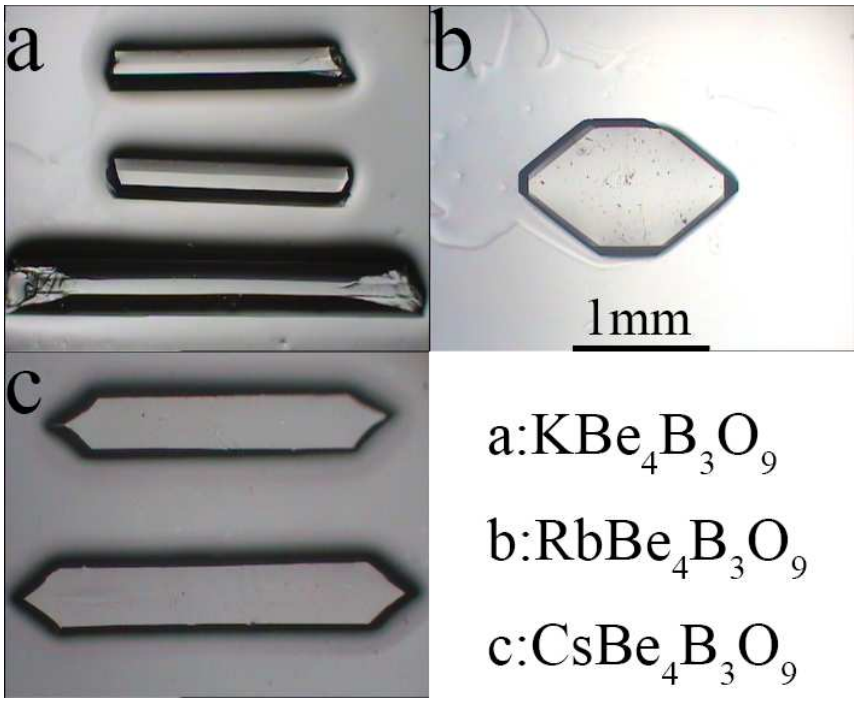

Fig 3. The crystal pictures of (a) $KBe_4B_3O_9$, (b) $RbBe_4B_3O_9$ and (c) $CsBe_4B_3O_9$

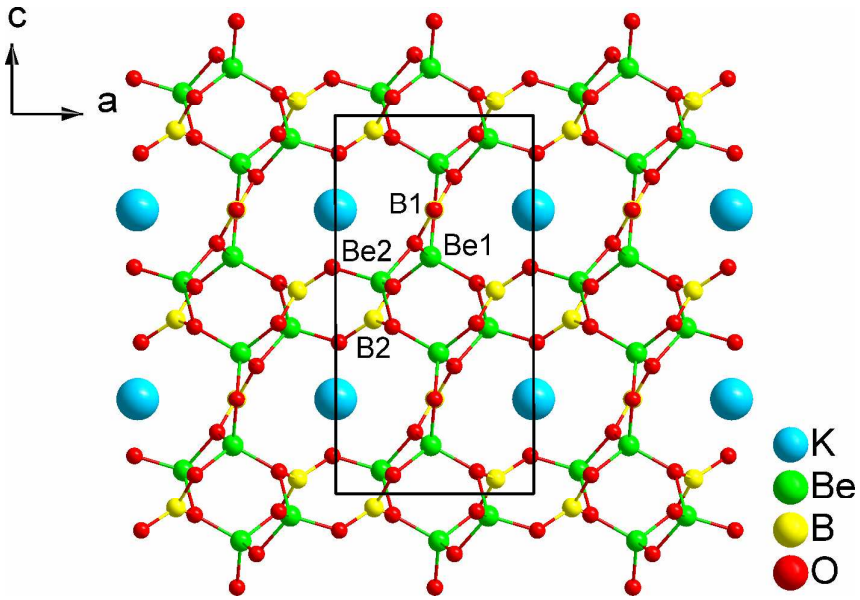

Fig 4. Crystal structure of $KBe_4B_3O_9$

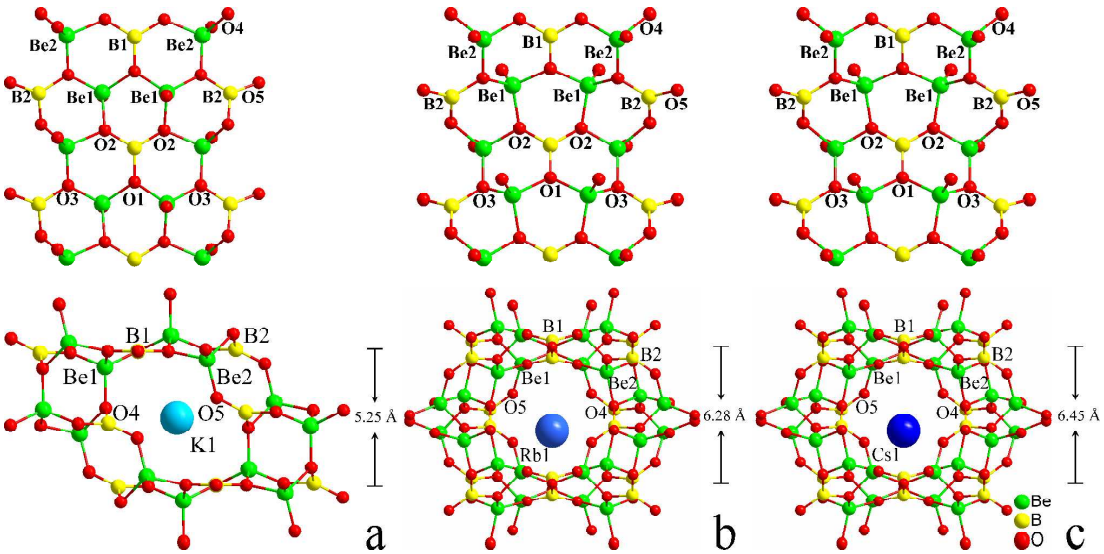

Fig 5. Structural evolution from $KBe_4B_3O_9$ to $ABe_4B_3O_9$ (A = Rb and Cs)

TOC

A New Alkaline Beryllium Borate $KBe_4B_3O_9$ with ribbon alveolate $[Be_2BO_5]_\infty$ layers and the structural evolution of $ABe_4B_3O_9$ (A = K, Rb and Cs)

Shichao Wang, Ning Ye* and Guohong Zou

A new alkaline beryllium borates $KBe_4B_3O_9$ consist of 2D ribbon alveolate beryllium borate $[Be_2BO_5]_\infty$ layers connected by strong covalent bonds.